

July 1996
revised October 1996
quant-ph/9611005

QUANTUM MECHANICS OF LATTICE GAS AUTOMATA

I. ONE PARTICLE PLANE WAVES AND POTENTIALS

David A. Meyer

*Institute for Physical Sciences
and
Project in Geometry and Physics
Department of Mathematics
University of California/San Diego
La Jolla, CA 92093-0112
dmeyer@chonji.ucsd.edu*

ABSTRACT

Classical lattice gas automata effectively simulate physical processes such as diffusion and fluid flow (in certain parameter regimes) despite their simplicity at the microscale. Motivated by current interest in quantum computation we recently defined *quantum* lattice gas automata; in this paper we initiate a project to analyze which physical processes these models can effectively simulate. Studying the single particle sector of a one dimensional quantum lattice gas we find discrete analogues of plane waves and wave packets, and then investigate their behaviour in the presence of inhomogeneous potentials.

PACS numbers: 03.65.-w, 02.70.-c, 11.55.Fv, 89.80.+h.

KEY WORDS: quantum lattice gas; quantum cellular automaton; quantum computation.

Phys. Rev. E **55** (1997) 5261–5269.

1. Introduction

The first quantum lattice gas automaton (QLGA) appeared as Feynman’s path integral for a relativistic particle in $1 + 1$ dimensions [1]; independently Riazanov constructed a $2 + 1$ dimensional QLGA as the path integral for the next higher dimensional Dirac equation [2]. In these formulations the quantum particle is conceptualized as evolving along spacetime trajectories, each of which is assigned a probability amplitude which is the product of a sequence of ‘scattering’ amplitudes describing the evolution of the particle during a single timestep. Thus these QLGA are discretizations of quantum mechanical processes.

Feynman’s path integral formulation of quantum mechanics reproduces the standard Schrödinger formulation of wave functions obeying partial differential equations [1]. These differential equations can be discretized directly, giving equations which Succi and Benzi naturally identify in the lattice gas paradigm as quantum lattice Boltzmann equations [3]. It is a familiar, although not often useful, observation that any numerical evolution of a discretized partial differential equation can be interpreted as the evolution of some cellular automaton (CA), if one allows the set of states to be \mathbb{R} , or \mathbb{C} , or \mathbb{Z}_N for some very large N . Taking this perspective, Bialynicki-Birula constructs a model for quantum evolution—a linear unitary CA [4]—which is essentially equivalent to, although derived independently of, Succi and Benzi’s equations.

The equivalence of a QLGA simulation and the evolution of a set of quantum lattice Boltzmann equations/unitary CA depends on the equivalence of the path integral and standard formulations of quantum mechanics in the continuum. Our recent work explaining the necessity of non-unitarity in earlier attempts of Grössing, Zeilinger, *et al.* to construct homogeneous CA for quantum evolution [5] demonstrates this equivalence directly for the discrete models [6]. We also note that, in contrast to simulation with deterministic or probabilistic LGA, simulation with a QLGA *requires* evolution along all possible spacetime trajectories. This may be achieved (slowly) by evolution of the quantum lattice Boltzmann equation on a classical computer or, at present hypothetically (but rapidly), by simulation on a quantum computer.

In fact, given the arguments that massive parallelism will optimize nanoscale quantum computer architecture [7], it is plausible that the first useful *quantum computation* [8] will implement a QLGA simulation of some quantum mechanical process. This provides two reasons to pursue the project described in this series of papers: we want to explore not only quantum mechanical phenomena which can be simulated effectively by QLGA, but also how well, as Feynman suggested [9], a quantum computer might simulate physics. In addition, we expect the quantum mechanics of LGA to have implications for discrete models of fundamental physics: we have already found remarkable consequences of unitarity in linear [6,10] and nonlinear [11] QCA.

We begin in the next section by recalling the model of [6] with which we will be working: the most general one dimensional homogeneous QLGA with a single particle of speed no more than 1 in lattice units. The local evolution rule for this model has *two* free

parameters: essentially the second measures the coupling between two copies of Feynman's original QLGA in which the first measures the 'mass' of the particle.

This generalized QLGA is exactly solvable, just as is a single Feynman QLGA. In Section 3 we demonstrate this by finding the discrete analogues of plane waves in, and the dispersion relation for, our QLGA. We also show the results of simulations of the former—on a *deterministic* computer.

We might imagine a one particle QLGA being simulated *quantum mechanically* by a ballistic electron in a solid state lattice [12] or as the 'low energy' sector of a line of dynamical quantum spins [9] ('low energy' meaning, *e.g.*, the configurations with one spin up and the rest down). In the former case [13], and certainly if our interest is in the QLGA as a discrete approximation to the Dirac equation [6], it is natural to investigate wave packets representing a semi-classical quantum particle. We do so in Section 4.

In Section 5 we show how to introduce an inhomogeneous potential into the model. Concentrating on finite square well potentials, we determine the dependence of the frequency/energy eigenvalues on the depth of the well and find that the eigenfunctions take the expected form. Finally, we utilize the results of Section 4 and show the results of simulations of a wave packet in a finite square well.

We summarize our results in Section 6 and indicate the directions in which this research is continuing.

2. The one particle QLGA

A lattice gas automaton (LGA) should be envisioned as a collection of particles moving synchronously from vertex to vertex on a fixed graph (lattice) L : At the beginning of each timestep each particle is located at some vertex and is labelled with a 'velocity' indicating along which edge incident to that vertex it will move during the 'advection' half of the timestep. After moving along the designated edge to the next vertex, in the 'scattering' half of the timestep the particles at each vertex interact according to some rule which assigns new 'velocity' labels to each. For the purposes of this paper we will consider only one dimensional lattices L , isomorphic to the integer lattice \mathbb{Z} or some periodic quotient thereof. In this case there are only two possible 'velocities': left and right. We will further restrict our attention to LGA with only a single particle; for some preliminary work on QLGA with multiple particles, see [6,14,15].

A QLGA is a LGA for which the time evolution is unitary. To make this precise we must first identify the Hilbert space of the theory. For a one particle QLGA in one dimension an orthonormal basis for the Hilbert space H is given by $|x, \alpha\rangle$ (in the standard Dirac notation [16]), where $x \in L$ denotes position and $\alpha \in \{\pm 1\}$ denotes 'velocity'. At each time the state of the QLGA is described by a *state vector* in H :

$$\Psi(t) = \sum_{x, \alpha} \psi_{\alpha}(t, x) |x, \alpha\rangle, \quad (2.1)$$

where the amplitudes $\psi_\alpha(t, x) \in \mathbb{C}$ and the norm of $\Psi(t)$, as measured by the inner product on H , is:

$$1 = \sum_{x, \alpha} \overline{\psi_\alpha(t, x)} \psi_\alpha(t, x). \quad (2.2)$$

The state vector evolves unitarily, *i.e.*, $\Psi(t+1) = U\Psi(t)$, where U is a unitary operator on H . Since the evolution is unitary, the inner product is preserved and (2.2) holds for all times if it holds for one; this allows the interpretation of $\overline{\psi_\alpha(t, x)} \psi_\alpha(t, x)$ as the probability that the particle be in the state $|x, \alpha\rangle$ at time t [16,17]. As usual, therefore, the basis state vectors $\Psi = |x, \alpha\rangle$ correspond to ‘classical’ states—with probability 1 there is a single particle at x with ‘velocity’ α —and a generic state vector (2.1) is a superposition of these ‘classical’ states, each of which has integer values (one 1, the rest 0) for the number of particles at each lattice site. (In general, the basis vectors for the n particle subspace of the QLGA Hilbert space are exactly the possible states of a classical deterministic LGA with n particles [15].)

In order for the evolution to have the ‘advection’ interpretation described above, the basis vectors should evolve so that

$$\langle x, \alpha | U | y, \beta \rangle \neq 0 \quad (2.3)$$

only when $x = y + \beta$. This is equivalent to a condition on the amplitudes:

$$\psi_\alpha(t+1, x) = f_\alpha(\psi_{-1}(t, x+1), \psi_{+1}(t, x-1)),$$

where taking f_α to be independent of x means that the QLGA is *homogeneous* in space. As the notation suggests, it is convenient to combine the left and right moving amplitudes at x into a two component complex vector $\psi(t, x) := (\psi_{-1}(t, x), \psi_{+1}(t, x))$ so that a state vector is written

$$\Psi(t) = \sum_x \psi(t, x) |x\rangle.$$

We showed in [6] that the most general unitary evolution for a one dimensional QLGA with parity invariance* is unitarily equivalent to

$$\psi(t+1, x) = \begin{pmatrix} 0 & i \sin \theta \\ 0 & \cos \theta \end{pmatrix} \psi(t, x-1) + \begin{pmatrix} \cos \theta & 0 \\ i \sin \theta & 0 \end{pmatrix} \psi(t, x+1), \quad (2.4)$$

up to some overall phase which has no physical effect. Here the parameter $\theta \in \mathbb{R}$, or more precisely, $\tan \theta$, plays a role something like ‘mass’: when $\theta = 0$ the particle travels only on the lightcone; as $\tan \theta$ increases its probability for moving more slowly does also.

Notice that just as in deterministic LGA in one dimension, the particle has a \mathbb{Z}_2 valued ‘Lagrangian’ conserved quantity measuring the parity of its fiducial space coordinate. This ‘spurious’ conserved quantity partitions the set of particles in a deterministic LGA into two

* *I.e.*, invariance under $x \rightarrow -x$; also called *reflection* invariance.

decoupled gases [18] and in the QLGA defined by (2.4) it partitions the set of amplitudes $\psi(t, x)$ into two independent sets according to $x+t \pmod{2}$. This motivates consideration of the most general, no less local model which breaks this symmetry, namely

$$\psi(t+1, x) = w_{-1}\psi(t, x-1) + w_0\psi(t, x) + w_{+1}\psi(t, x+1), \quad (2.5)$$

where $w_i \in M_2(\mathbb{C})$ are 2×2 complex matrices. In terms of the basis vectors $|x, \alpha\rangle$, now (2.3) holds when $x = y + \beta$ or $x = y$, *i.e.*, the particle can have nonzero amplitude to maintain its position. The condition that the global evolution, *i.e.*, the matrix U , be unitary is expressed in terms of the w_i by the equations:

$$\begin{aligned} w_{-1}w_{-1}^\dagger + w_0w_0^\dagger + w_{+1}w_{+1}^\dagger &= I \\ w_0w_{-1}^\dagger + w_{+1}w_0^\dagger &= 0 \\ w_{+1}w_{-1}^\dagger &= 0, \end{aligned} \quad (2.6)$$

together with their Hermitian conjugates [6]. Imposing also the condition of parity (reflection) invariance on evolution of the form (2.5), we showed in [6] that the most general solution, up to unitary equivalence and an overall phase, is given by

$$\begin{aligned} w_{-1} &= \cos \rho \begin{pmatrix} 0 & i \sin \theta \\ 0 & \cos \theta \end{pmatrix} & w_{+1} &= \cos \rho \begin{pmatrix} \cos \theta & 0 \\ i \sin \theta & 0 \end{pmatrix} \\ w_0 &= \sin \rho \begin{pmatrix} \sin \theta & -i \cos \theta \\ -i \cos \theta & \sin \theta \end{pmatrix}. \end{aligned} \quad (2.7)$$

Here $\rho \in \mathbb{R}$ is a coupling parameter breaking the ‘spurious’ symmetry. When $\rho = 0$, (2.5) reduces to (2.4), the QLGA which is unitarily equivalent to the models of Feynman [1], Succi and Benzi [3], and Bialynicki-Birula [4]. As $\tan \rho$ increases, the relative weight of w_0 increases and the particle has greater probability of maintaining its position, *i.e.*, having zero velocity. This is the first indication of a symmetry between θ and ρ which will become more explicit as we investigate the general QLGA of (2.5) and (2.7).

3. Plane waves

The local evolution rule (2.5) is linear so we expect the model to be exactly solvable. In [6] we solved the $\rho = 0$ case by counting spacetime lattice paths in order to compute the *propagator* $K_{\alpha\beta}(t, x; 0, 0) := \langle x, \alpha | U^t | 0, \beta \rangle$ explicitly. Lattice paths are more difficult to count when the particle has nonzero amplitudes for maintaining its position during each timestep. Avoiding this difficulty leads us to a more physical approach—finding the discrete analogue of plane waves in a QLGA.

Recall that the QLGA is homogeneous, *i.e.*, U commutes with the translation (shift) operator T defined by $(T\psi)(x) := \psi(x+1)$. Suppose $L = \mathbb{Z}_N$. Then the eigenvalues of T are e^{ik} for wave numbers $k = 2\pi n/N$, $n \in \{0, \dots, N-1\}$, and the corresponding eigenvectors $\Psi^{(k)}$ satisfy:

$$\psi^{(k)}(x+1) = e^{ik}\psi^{(k)}(x). \quad (3.1)$$

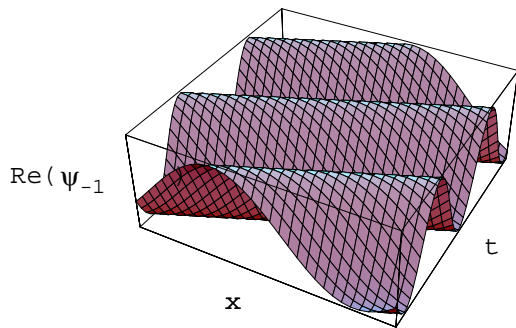


Figure 1. Evolution of the $n = 1$ right moving plane wave on a periodic lattice with $\theta = \pi/3$ and $\rho = \pi/4$.

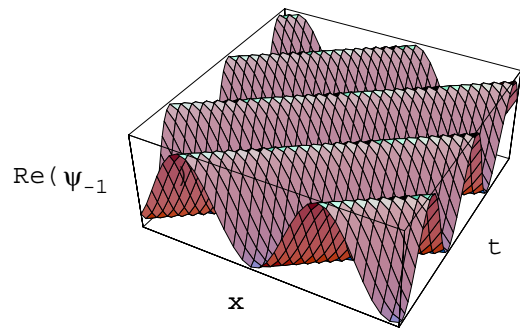


Figure 2. Evolution of the $n = 2$ right moving plane wave on a periodic lattice with $\theta = \pi/3$ and $\rho = \pi/4$.

Since $[U, T] = 0$ and U is unitary, the $\Psi^{(k)}$ are also eigenvectors for U with

$$U\Psi^{(k)} = e^{-i\omega_k}\Psi^{(k)}, \quad (3.2)$$

for some frequencies $\omega_k \in \mathbb{R}$. The eigenvectors $\Psi^{(k)}$ are the discrete analogues of plane waves since they evolve simply by phase multiplication.

Since the action of U is defined by (2.5), (3.1) and (3.2) imply that

$$\begin{aligned} e^{-i\omega_k}\psi^{(k)}(x) &= w_{-1}\psi^{(k)}(x-1) + w_0\psi^{(k)}(x) + w_{+1}\psi^{(k)}(x+1) \\ &= (e^{-ik}w_{-1} + w_0 + e^{ik}w_{+1})\psi^{(k)}(x) \\ &=: D(k)\psi^{(k)}(x). \end{aligned} \quad (3.3)$$

Thus the $e^{-i\omega_k}$ are eigenvalues of $D(k) \in M_2(\mathbb{C})$, *i.e.*, solutions of

$$\det(D(k) - e^{-i\omega_k}I) = 0, \quad (3.4)$$

where I is the 2×2 identity matrix. Using the parametrization (2.7) of the w_i , (3.4) reduces to the condition

$$\cos \omega = \cos k \cos \theta \cos \rho + \sin \theta \sin \rho. \quad (3.5)$$

For a given wave number k , (3.5) determines two frequencies $\pm\omega_k$ in terms of the rule parameters θ and ρ . Call the corresponding eigenvectors of $D(k)$ (normalized to have length $1/N$) $\psi^{(k,\pm 1)}(0) \in \mathbb{C}^2$, so that the corresponding plane waves are defined by (3.1) to be

$$\Psi^{(k,\epsilon)} := \sum_x \psi^{(k,\epsilon)}(0)e^{ikx}|x\rangle. \quad (3.6)$$

Figures 1 and 2 show the evolution of $\epsilon = +1$ (right moving) plane waves for $n = 1, 2$. The probability $\psi^\dagger(t, x)\psi(t, x)$ (where $\psi^\dagger(t, x) := {}^t\psi(t, x)$) of the particle being at x is constant in x (and t), so the vertical axis in the graphs shows the real part of $\psi_{-1}(t, x)$. Even on such a small ($N = 32$) lattice this QLGA provides a very good approximation to continuum plane waves of long wavelength measured in lattice units.

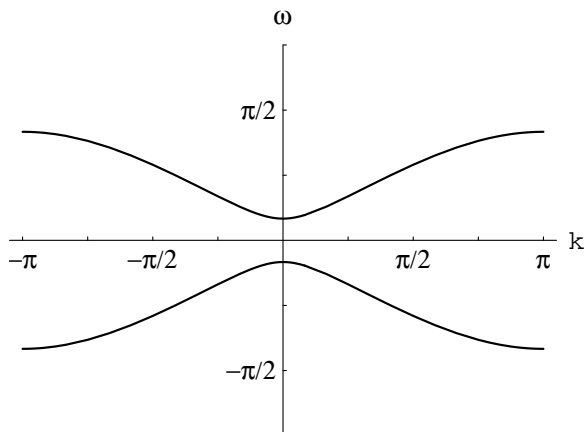


Figure 3. The dispersion relation for $\theta = \pi/3$ and $\rho = \pi/4$. $\pi/12 \leq |\omega| \leq 5\pi/12$.

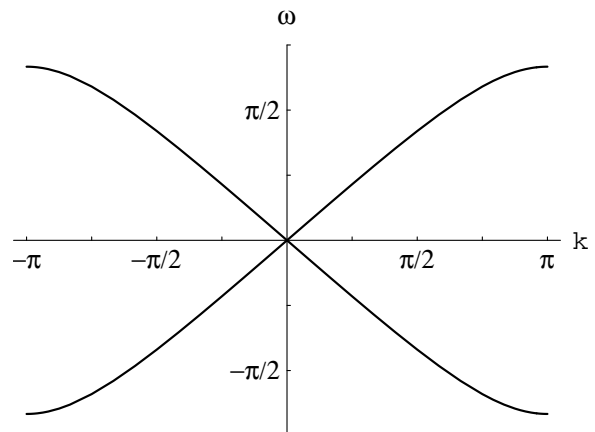


Figure 4. The dispersion relation in the ‘massless’ case $\theta = \rho = \pi/6$. $|\omega| \leq 2\pi/3$.

Notice that when the wave number k increases, so does the frequency ω —the time period is shorter in Figure 2 than in Figure 1. Also the *phase velocity* ω/k decreases—the crest of the wave moves more slowly. In fact, (3.5) is the exact *dispersion relation*, giving the frequency in terms of the wave number. Figure 3 graphs the dispersion relation for the QLGA with the same rule parameters used in the simulations of Figures 1 and 2. The graph has reflection symmetry about both axes since (3.5) is invariant under both $k \rightarrow -k$ and $\omega \rightarrow -\omega$. Each reflection alone changes the direction of the plane wave. When $k = 0$, $\omega = \pm(\theta - \rho)$; when $k = \pm\pi$, $\omega = \pm(\theta + \rho - \pi)$. These values exemplify another symmetry of the dispersion relation—invariance under $\theta \leftrightarrow \rho$; this is a symmetry in the QLGA rule space which is not realizable by a *local* unitary transformation. Figure 4 graphs the special case of equal rule parameters; here the dispersion relation passes through the origin.

By comparison with plane waves in continuum quantum mechanics [16,17], we know that ω and k should be interpreted as being proportional to *energy* and *momentum*, respectively. Expanding the dispersion relation (3.5) around $k = 0$ and $\omega = 0$ to second order, we find

$$\omega^2 = k^2 \cos \theta \cos \rho + 2(1 - \cos(\theta - \rho)). \quad (3.7)$$

For a relativistic particle in the continuum,

$$E^2 = p^2 c^2 + m^2 c^4. \quad (3.8)$$

Comparing (3.7) and (3.8) suggests that the $1 - \cos(\theta - \rho) = 0$ case, *i.e.*, the $\theta = \rho$ case shown in Figure 4, corresponds to the particle being *massless*.

Not only do the plane wave parameters ω and k bear the interpretation of proportionality to the conserved quantities energy and momentum, but they also label a complete set of (nonlocal) conserved quantities for the QLGA. Since T is orthogonal its eigenvectors $\Psi^{(k,\epsilon)}$ are orthogonal for distinct wave numbers k . Furthermore, $D(k)$ is unitary, so its

eigenvectors $\psi^{(k,\pm 1)}(0)$ are orthogonal for each k and hence so are the plane waves $\Psi^{(k,\pm 1)}$. Since we normalized the eigenvectors of $D(k)$ to have length $1/N$, the plane waves (3.6) form an orthonormal basis for H which we denote by $\{|k, \epsilon\rangle\}$. Consider any state vector $\Psi \in H$:

$$\begin{aligned}\Psi &= \sum_x \psi(x) |x\rangle \\ &= \sum_x \psi(x) \sum_{k, \epsilon} |k, \epsilon\rangle \langle k, \epsilon | x \rangle \\ &= \sum_{k, \epsilon} \left(\sum_x \langle k, \epsilon | x \rangle \psi(x) \right) |k, \epsilon\rangle\end{aligned}$$

The parenthesized expression is the amplitude of $|k, \epsilon\rangle$ in the new basis:

$$\begin{aligned}\hat{\psi}_\epsilon(k) &:= \sum_x \langle k, \epsilon | x \rangle \psi(x) \\ &= \sum_x \left(\sum_y \psi^{(k, \epsilon)}(0) e^{iky} |y\rangle \right)^\dagger |x\rangle \psi(x) \\ &= (\psi^{(k, \epsilon)}(0))^\dagger \sum_x \psi(x) e^{-ikx} \\ &=: (\psi^{(k, \epsilon)}(0))^\dagger \hat{\psi}(k),\end{aligned}\tag{3.9}$$

where $\hat{\psi}(k)$ is the *discrete Fourier transform* of $\psi(x)$. The plane waves $|k, \epsilon\rangle$ evolve by phase multiplication so the probabilities $\hat{\psi}_\epsilon(k) \hat{\psi}_\epsilon(k)$ are left invariant by the evolution. Since any initial state vector $\Psi(0)$ can be expressed in the plane wave basis this way, the existence of these conserved quantities is equivalent to exact solvability for this model of a one particle QLGA.

4. Wave packets

The plane waves (3.6) provide a starting point for constructing wave packets with localized position and particularized momentum. Consider the right moving plane wave with wave number k_0 in the position basis:

$$\Psi^{(k_0, +1)} = \sum_x \psi^{(k_0, +1)}(0) e^{ik_0 x} |x\rangle.$$

In this discrete (and periodic) situation the binomial distribution is a convenient substitute for a Gaussian distribution, so to localize the particle we multiply the amplitudes by appropriate binomial coefficients: Let

$$\Psi := \binom{2s}{s}^{-1} \sum_x \psi^{(k_0, +1)}(0) e^{ik_0 x} \binom{s}{x - x_0 + s/2} |x\rangle,\tag{4.1}$$

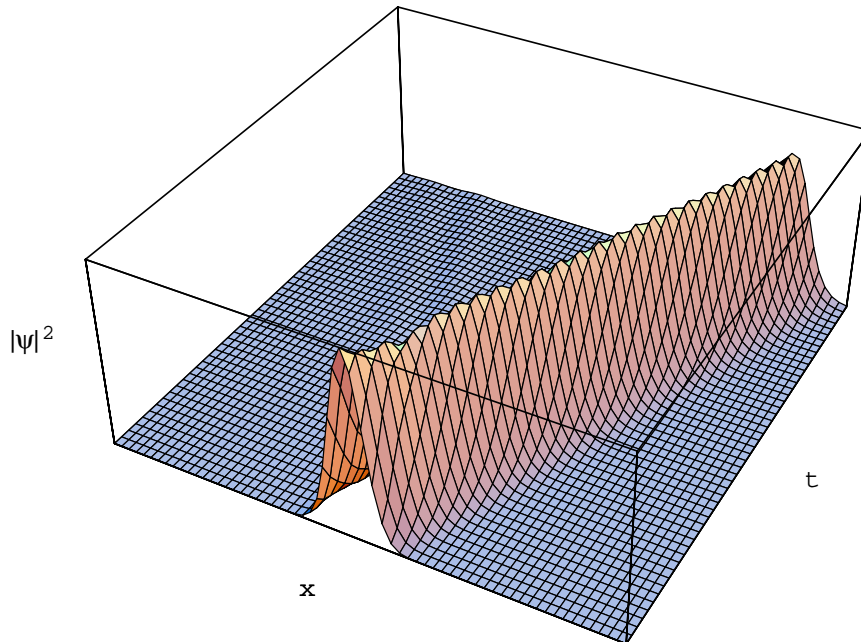


Figure 5. Evolution of the $k_0 = \pi/4$ wave packet (4.1) with width $s = 32$ for rule parameters $\theta = \pi/3$, $\rho = \pi/4$. The probability peak moves from $x = 31$ at $t = 0$ to $x = 54$ at $t = 49$; thus the group velocity is approximately $23/49 \approx 0.47$.

for even $s \leq N$, where the inverse binomial coefficient outside the sum is the requisite normalization factor. This wave packet is localized around x_0 , having support on the interval $[x_0 - s/2, x_0 + s/2]$. Figure 5 shows the evolution for wave number $k_0 = \pi/4$ and width $s = 32$ on the lattice \mathbb{Z}_{64} . The rule parameters are the same as those used in the simulations shown in Figures 1 and 2. In contrast to those graphs, the vertical axis in Figure 5 shows the probability that the particle is in the state $|x\rangle$.

This simulation shows that the $k_0 = \pi/4$ wave packet moves with well defined *group velocity* to the right. The result is just what we would expect by analogy with the continuum situation and can be analyzed in the same way, by transforming to the $|k, \epsilon\rangle$ basis. Using (3.9) we compute the amplitudes in this basis:

$$\begin{aligned}
 \hat{\psi}_\epsilon(k) &= (\psi^{(k, \epsilon)}(0))^\dagger \binom{2s}{s}^{-1} \sum_x \psi^{(k_0, +1)}(0) e^{ik_0 x} \binom{s}{x - x_0 + s/2} e^{-ikx} \\
 &= (\psi^{(k, \epsilon)}(0))^\dagger \psi^{(k_0, +1)}(0) \binom{2s}{s}^{-1} \sum_x \binom{s}{x - x_0 + s/2} e^{i(k_0 - k)x} \\
 &= (\psi^{(k, \epsilon)}(0))^\dagger \psi^{(k_0, +1)}(0) \binom{2s}{s}^{-1} e^{i(k_0 - k)(x_0 - s/2)} (1 + e^{i(k_0 - k)})^s \\
 &= (\psi^{(k, \epsilon)}(0))^\dagger \psi^{(k_0, +1)}(0) \binom{2s}{s}^{-1} e^{i(k_0 - k)x_0} 2^s \cos^s \left(\frac{k_0 - k}{2} \right) \tag{4.2}
 \end{aligned}$$

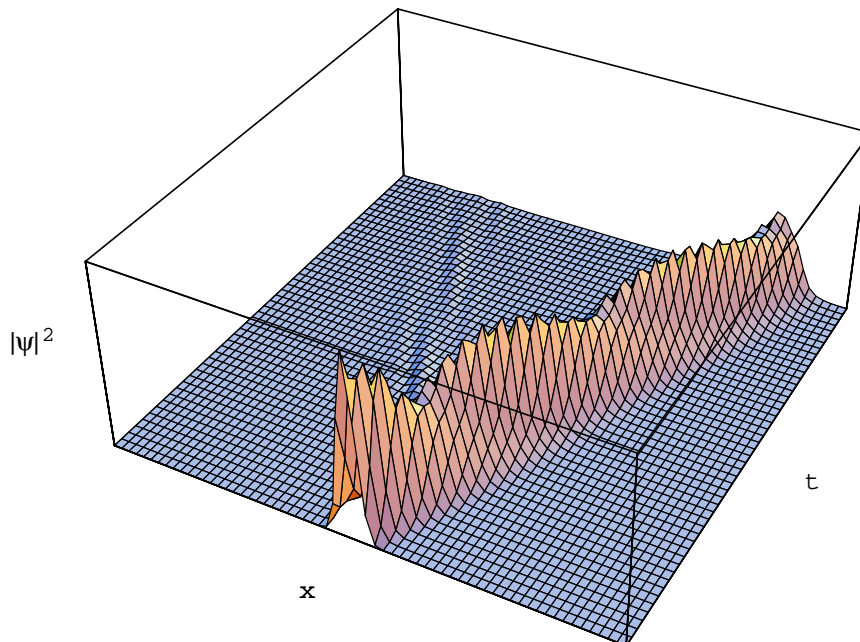


Figure 6. Evolution of the $k_0 = \pi/4$ wave packet (4.1) with width $s = 8$ for rule parameters $\theta = \pi/3$, $\rho = \pi/4$. This wave packet disperses more rapidly than the one shown in Figure 5: The peak probability at the end of the simulation is less than half of the initial peak probability; left moving ripples carrying off some of the probability are also visible.

The amplitudes (4.2) give probabilities peaked around $k = k_0$, so this is also a wave packet in momentum space. As usual, the group velocity is the slope of the dispersion relation (3.5), *i.e.*, $d\omega/dk|_{k_0}$, which is $\sqrt{9 - 2\sqrt{6}}/4 \approx 0.49$ for the values used in the simulation of Figure 5; this is in good agreement with the measured value of approximately 0.47.

The width of the peak in (4.2) depends inversely on s : as s decreases, *i.e.*, the width of the wave packet in position space decreases, the width of the momentum peak increases. The simulation in Figure 6 shows the evolution of a wave packet with width $s = 8$. We note that while the group velocity is the same as in Figure 5, there is substantially more dispersion, indicating a greater interval of contributing wave numbers. This is a general result, not depending on the specific form of our wave packet; the *reciprocity relation* for the discrete Fourier transform has consequences similar to those of the uncertainty relation for the continuous Fourier transform [19].

Figure 7 shows a simulation of a wave packet built from the plane wave with smallest nonzero wave number on the \mathbb{Z}_{64} lattice: $k_0 = \pi/32$. The horizontal tangent to the graph of the dispersion relation at $k = 0$, as shown in Figure 3, indicates that the group velocity of this wave packet will be small. Furthermore, even with width $s = 32$ the wave number interval includes the left going modes whose presence is visible in Figure 7; the consequence is an interference pattern and no very well defined group velocity.

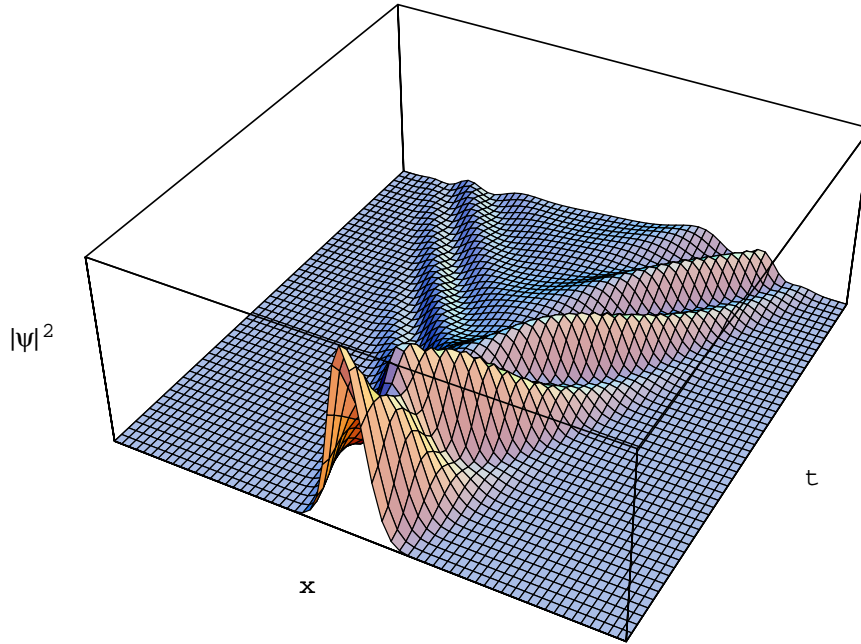


Figure 7. Evolution of the $k_0 = \pi/32$ wave packet (4.1) with width $s = 32$; the rule parameters are still $\theta = \pi/3$, $\rho = \pi/4$. This wave packet disperses even more rapidly than the one shown in Figure 6: left moving waves carry off some of the probability and an interference pattern is created.

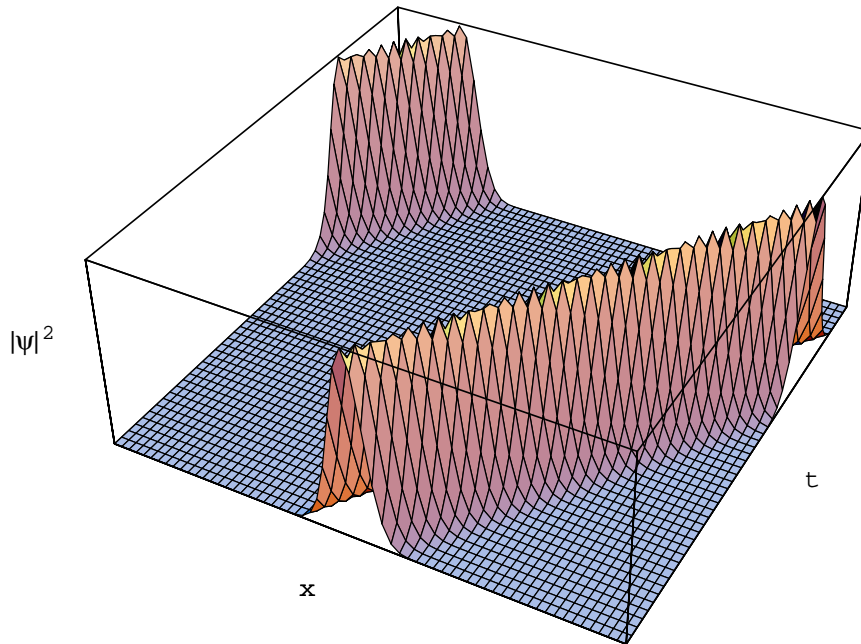


Figure 8. Evolution of the $k_0 = \pi/32$ wave packet (4.1) with width $s = 32$ for rule parameters $\theta = \pi/6 = \rho$. This wave packet disperses very little and has group velocity close to 1 in lattice units.

Finally, Figure 8 shows the evolution of the same wave packet but for the rule parameters $\theta = \pi/6 = \rho$ whose dispersion relation is graphed in Figure 4. Here the group velocity is close to 1 in lattice units, even for k_0 as small as $\pi/32$; the particle is indeed ‘massless’. There is almost no dispersion in this simulation; the probability contained in left going modes is nonzero, but too small by several orders of magnitude to be visible in Figure 8.

5. Potentials

The one particle QLGA described in Section 2 is the most general *homogeneous* model for particle speeds no more than 1. To simulate physical systems (or to do useful computation), some inhomogeneity must be introduced. In each of the equations (2.6), which express the unitarity condition, all the w_i correspond to the scattering/interaction at a single lattice point, as do all the w_i^\dagger . In the first equation these are the same lattice point, while in the second and third they are different. Thus if $w_i(x) = w_i$, constants independent of x , solve these equations, so do $e^{-i\phi(x)}w_i$. As observed already by Feynman [1] and Riazanov [2], such an x dependent phase realizes an inhomogeneous potential in the continuum limit of the discrete path sum for the Dirac equation. Here we investigate its effects on the quantum mechanics of our LGA, expecting them to be similar to those in the continuum limit.

For simplicity, we restrict our attention to a finite square well potential, *i.e.*,

$$w_i(x) := \begin{cases} e^{-i\phi}w_i & \text{if } N/4 \leq x < 3N/4; \\ w_i & \text{otherwise,} \end{cases}$$

where the w_i are defined by (2.7). We begin by considering the effect of different values for ϕ .

Recall that the frequency (or energy) eigenvalues ω are doubly degenerate except for those with the largest and smallest absolute value. (See Figure 3, where each horizontal line intersecting the graph of the dispersion relation does so at two points except when tangent to the maximum or minimum of either branch of the curve.) As with any perturbation to the evolution, we expect the introduction of an inhomogeneity in the potential to resolve the degenerate eigenvalues. Figure 9 shows that this is indeed the case: as ϕ increases away from 0 the eigenvalues ω of U increase and the degenerate ones split.

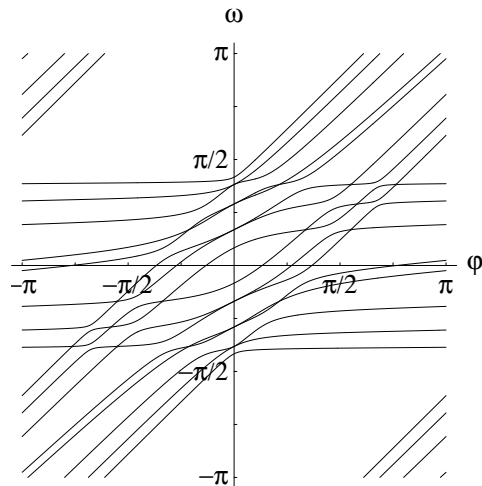


Figure 9. The eigenvalues ω of U for a square well of depth ϕ and width $N/2$ on a lattice of size $N = 8$ with $\theta = \pi/3$ and $\rho = \pi/4$.

The eigenvalues in Figure 9 have been computed for only $N = 8$; Figure 10 shows

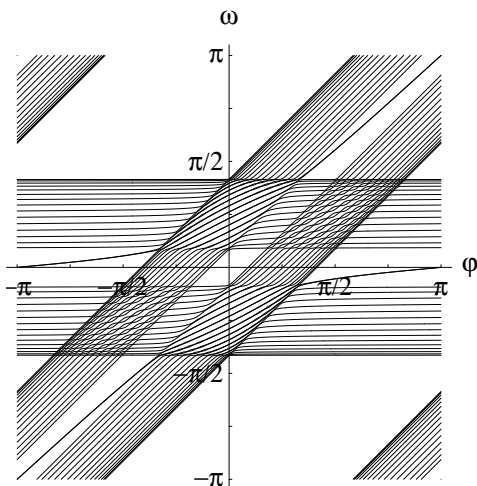


Figure 10. The eigenvalues ω of U for a square well of depth ϕ and width $N/2$ on a lattice of size $N = 32$ with $\theta = \pi/3$ and $\rho = \pi/4$.

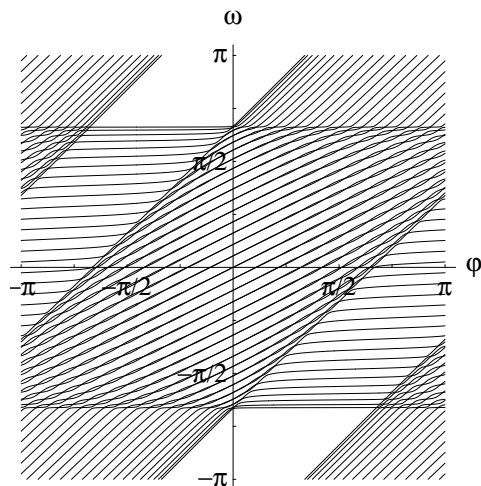


Figure 11. The eigenvalues ω of U for a square well of depth ϕ and width $N/2$ on a lattice of size $N = 32$ in the ‘massless’ case $\theta = \pi/6 = \rho$.

the results for $N = 32$. On the larger lattice it is clear what happens: the horizontal bands of frequency/energy eigenvalues correspond to the eigenvalues of the unperturbed, homogeneous system, while the diagonal bands of eigenvalues correspond to the same ones, but shifted by the depth ϕ of the square well. The periodicity along the frequency axis shown in these graphs is a symptom of the ambiguity in the definition of energy due to discrete time evolution [20]. The graphs in Figures 9 and 10 have been computed for the QLGA with parameter values $\theta = \pi/3$, $\rho = \pi/4$, the dispersion relation for which is shown in Figure 3. Repeating the calculations for the ‘massless’ case, with dispersion relation shown in Figure 4, gives the frequency/energy eigenvalue plot shown in Figure 11. The degenerate levels still split, but much less than before for the same ϕ values, and the part of the band structure resulting from the nonzero minimum positive frequency in the massive dispersion relation vanishes.

Now consider the eigenvectors of U , namely the eigenfunctions for our discrete version of a finite square well. Since U is no longer translation invariant we do not have an equation like (3.3) to solve for the eigenfunctions analytically. Rather than developing a cross boundary matching method as is used in the continuum problem for a periodic square well potential [21], here we simply find the eigenvectors of U numerically. Figure 12 shows the eigenfunctions corresponding to the three smallest positive eigenvalues for the QLGA with $\theta = \pi/3$ and $\rho = \pi/4$. The depth of the square well is $\phi = \pi/24$. We see exactly the lowest modes we would expect from our experience with such a potential in the continuum. As the energy of the eigenfunction increases there is greater probability that the particle is outside the well—in the region of higher potential. Figure 13 shows an eigenfunction which is approximately a plane wave in both regions: it has larger wave number in the well than outside it. For analytic results on the closely related problem of a step potential, and some discussion of their consequences for the physical interpretation of QLGA, see [15].

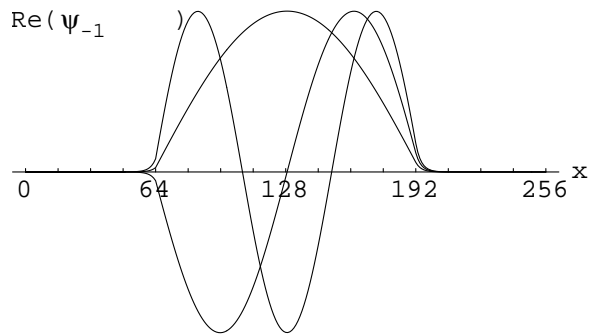


Figure 12. The three eigenfunctions of U with smallest positive eigenvalues: $\pi/12 < 0.2622 < 0.2634 < 0.2653$, for a square well of depth $\pi/24$ and width $N/2$ on a lattice of size $N = 256$ with $\theta = \pi/3$ and $\rho = \pi/4$.

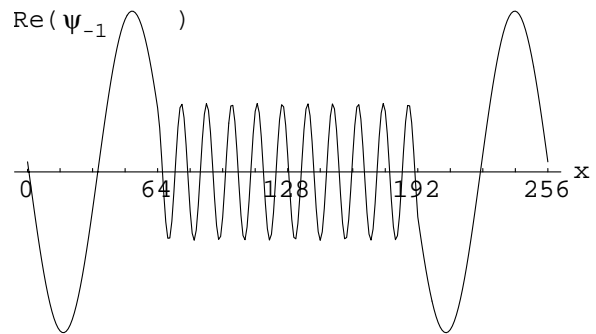


Figure 13. An eigenfunction for a particle with eigenvalue $0.3985 < 5\pi/12$ large enough not to be confined completely to the square well of the previous figure. Outside the square well the wave number decreases and the probability increases.

Finally, suppose we prepare one of the semiclassical wave packets studied in Section 4 in a finite square well. Using the dispersion relation (3.5), we find that the $k_0 = \pi/4$, width $s = 32$ wave packet (4.1) of Figure 5 has peak frequency $\omega_0 = \text{Cos}^{-1}((1 + \sqrt{6})/4)$ for rule parameters $\theta = \pi/3$, $\rho = \pi/4$. ω_0 is just a little larger than $\pi/6$ so we would not expect a square well of depth $\phi = \pi/6$ to contain this wave packet. Figure 14 shows a simulation of this situation on a lattice of size $N = 64$: the wave packet continues past the right edge of the square well at $3N/4$ with only a small amount of internal reflection.

Increasing the depth of the square well should have the effect of increasing the amount of internal reflection of the wave packet. Simulations demonstrate that this is indeed the case. When the depth of the square well is $\phi = \pi/4$, Figure 15 shows that the wave packet splits as it scatters off the right wall of the square well. With greater probability the particle is reflected back into the well, but it also has a substantial probability of continuing to the right. The wave packet which continues to the right does so at a reduced group velocity as we can see by the fact that the reflected wave packet travels back across the well, reaching the left wall at $x = N/4 = 16$ at the end of the simulation shown, before the transmitted wave packet travels the same distance rightwards.

Finally, when the depth of the square well is increased to $\phi = \pi/3$, Figure 16 shows that almost the entire wave packet is reflected back into the well by the right wall. In this case there is only a very small probability that the particle has sufficiently large energy to escape the well.

6. Discussion

Unitarity is a very restrictive constraint on the local scattering rule for a QLGA with a single particle of bounded speed. When the bound is 1 in lattice units, there is a two parameter family of reflection invariant one dimensional local rules, given by (2.5) and (2.7). It is already remarkable that the Dirac equation arises as a continuum limit of this QLGA

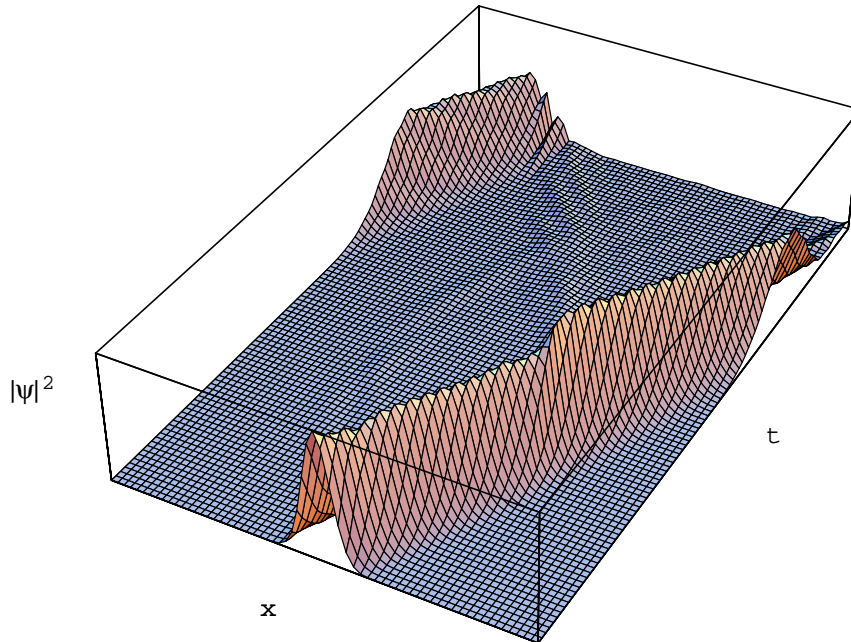


Figure 14. Evolution of the $k_0 = \pi/4$ wave packet (4.1) with width $s = 32$ for rule parameters $\theta = \pi/3$, $\rho = \pi/4$ in a square well of depth $\phi = \pi/6$. There is very little reflection as the wave packet passes the right wall of the square well at $x = 3N/4 = 48$.

when $\rho = 0$. In this paper we have begun to investigate the quantum mechanics of the general two parameter rule. We find that *even without going to a continuum limit* the QLGA reproduces the quantum mechanical phenomena of plane waves and wave packets obeying a dispersion relation (3.5). Furthermore, the model straightforwardly accommodates the inclusion of inhomogeneous potentials. The eigenvectors of the evolution matrix give the quantum mechanical eigenfunctions for the lattice gas particle, and simulations exhibit the semi-classical evolution of a wave packet, in the presence of a square well potential.

Taking a QLGA seriously as a possible model for quantum computation by, for example, ballistic electrons in a lattice of solid state nanostructures, raises many additional questions, some of which will be addressed in subsequent papers in this series: Inhomogeneity of the substrate can be incorporated in the model by varying the rule parameters while maintaining global unitarity. Finite, non-periodic, boundary conditions can be imposed similarly [22]. Higher dimensional [2,4,10,14] and multiparticle [6,14,17] models can also be constructed. Decoherence is the crucial problem for quantum computers [8], particularly in the solid state [23]. QLGA provide an extremely convenient arena in which to model this problem [24]. Finally, the question of for which quantum computational tasks QLGA are best suited deserves serious investigation.

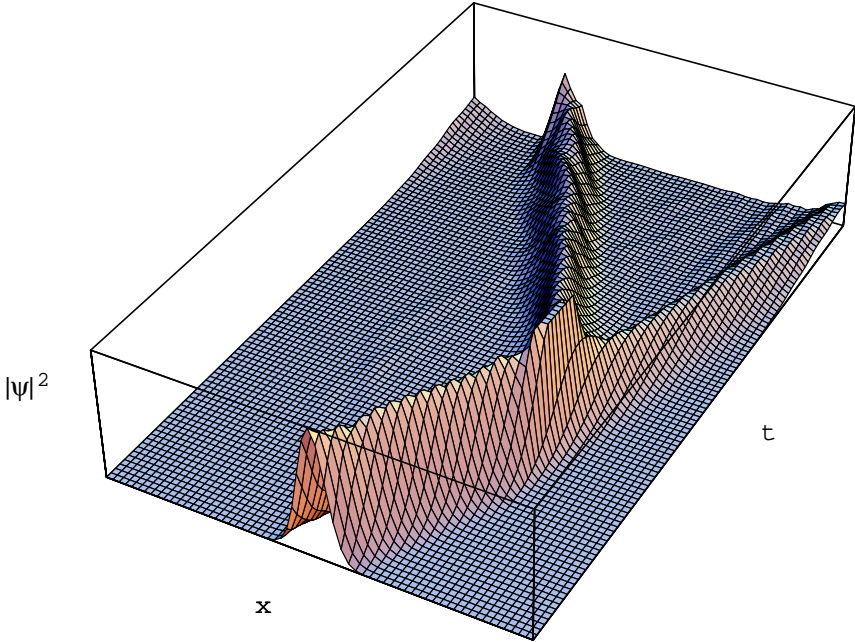


Figure 15. Evolution of the same wave packet with the same rule parameters as in Figure 14, but now in a square well of depth $\phi = \pi/4$. There is both reflection and transmission as the wave packet scatters off the right wall of the square well.

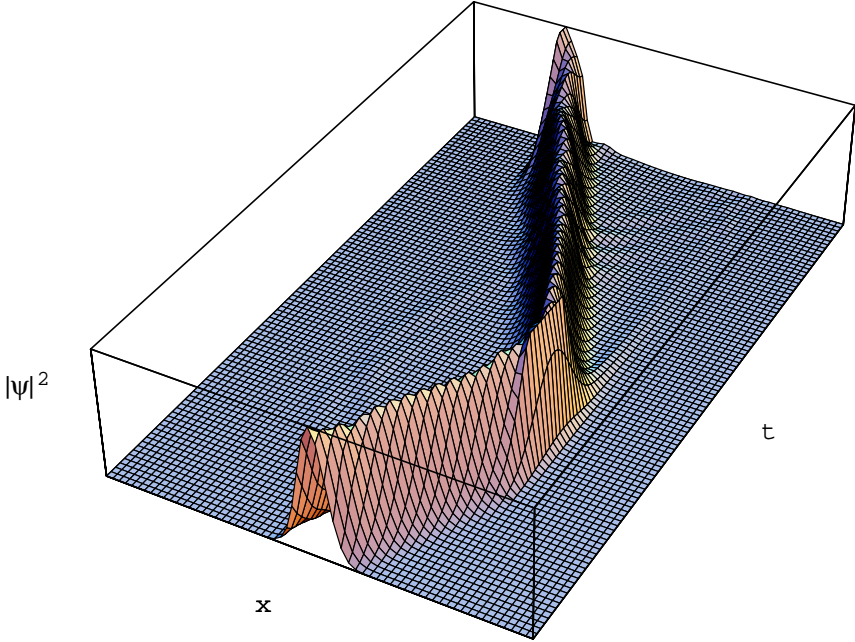


Figure 16. Evolution of the same wave packet with the same rule parameters as in Figures 14 and 15, but now in a square well of depth $\phi = \pi/3$. This well is deep enough that the wave packet is almost entirely reflected by the right wall of the square well.

Acknowledgements

It is a pleasure to thank Peter Doyle, Mike Freedman, Peter Monta and Richard Stong for discussions on various aspects of this project. I also benefited from conversations with Herbert Bernstein, Thomas Beth, Päivi Törmä and Harald Weinfurter at the 4th Workshop on Quantum Computation sponsored by the ISI Foundation.

References

- [1] R. P. Feynman and A. R. Hibbs, *Quantum Mechanics and Path Integrals* (New York: McGraw-Hill 1965).
- [2] G. V. Riazanov, “The Feynman path integral for the Dirac equation”, *Sov. Phys. JETP* **6** (1958) 1107–1113.
- [3] S. Succi and R. Benzi, “Lattice Boltzmann equation for quantum mechanics”, *Physica D* **69** (1993) 327–332;
S. Succi, “Numerical solution of the the Schrödinger equation using discrete kinetic theory”, *Phys. Rev. E* **53** (1996) 1969–1975.
- [4] I. Bialynicki-Birula, “Weyl, Dirac, and Maxwell equations on a lattice as unitary cellular automata”, *Phys. Rev. D* **49** (1994) 6920–6927.
- [5] G. Grössing and A. Zeilinger, “Quantum cellular automata”, *Complex Systems* **2** (1988) 197–208;
S. Fussy, G. Grössing, H. Schwabl and A. Scrinzi, “Nonlocal computation in quantum cellular automata”, *Phys. Rev. A* **48** (1993) 3470–3477;
and references therein.
- [6] D. A. Meyer, “From quantum cellular automata to quantum lattice gases”, *J. Stat. Phys.* **85** (1996) 551–574.
- [7] W. D. Hillis, “New computer architectures and their relationship to physics or why computer science is no good”, *Int. J. Theor. Phys.* **21** (1982) 255–262;
N. Margolus, “Parallel quantum computation”, in W. H. Zurek, ed., *Complexity, Entropy, and the Physics of Information*, proceedings of the SFI Workshop, Santa Fe, NM, 29 May–10 June 1989, *SFI Studies in the Sciences of Complexity VIII* (Redwood City, CA: Addison-Wesley 1990) 273–287;
B. Hasslacher, “Parallel billiards and monster systems”, in N. Metropolis and G.-C. Rota, eds., *A New Era in Computation* (Cambridge: MIT Press 1993) 53–65;
R. Mainieri, “Design constraints for nanometer scale quantum computers”, preprint (1993) LA-UR 93-4333, cond-mat/9410109;
M. Biafore, “Cellular automata for nanometer-scale computation”, *Physica D* **70** (1994) 415–433.
- [8] D. P. DiVincenzo, “Quantum computation”, *Science* **270** (1995) 255–261;
I. L. Chuang, R. Laflamme, P. W. Shor and W. H. Zurek, “Quantum computers, factoring, and decoherence”, *Science* **270** (1995) 1633–1635;
A. Barenco and A. Ekert, “Quantum computation”, *Acta Physica Slovaca* **45** (1995) 1–12;
and references therein.

- [9] R. P. Feynman, “Simulating physics with computers”, *Int. J. Theor. Phys.* **21** (1982) 467–488.
- [10] D. A. Meyer, “On the absence of homogeneous scalar unitary cellular automata”, UCSD preprint (1995), quant-ph/9604011, to appear in *Phys. Lett. A*.
- [11] C. Dürr, H. Lê Thanh and M. Santha, “A decision procedure for well-formed linear quantum cellular automata”, in C. Puecha and R. Reischuk, eds., *STACS 96: Proceedings of the 13th Annual Symposium on Theoretical Aspects of Computer Science*, Grenoble, France, 22–24 February 1996, *Lecture notes in computer science* **1046** (New York: Springer-Verlag 1996) 281–292;
 C. Dürr and M. Santha, “A decision procedure for unitary linear quantum cellular automata”, preprint (1996), quant-ph/9604007;
 D. A. Meyer, “Unitarity in one dimensional nonlinear quantum cellular automata”, UCSD preprint (1996), quant-ph/9605023;
 W. van Dam, “A universal quantum cellular automaton”, preprint (1996).
- [12] R. P. Feynman, “Quantum mechanical computers”, *Found. Phys.* **16** (1986) 507–531.
- [13] P. Benioff, “Quantum ballistic evolution in quantum mechanics: application to quantum computers”, preprint (1996), quant-ph/9605022.
- [14] B. M. Boghosian and W. Taylor, IV, “A quantum lattice-gas model for the many-particle Schrödinger equation in d dimensions”, preprint (1996) BU-CCS-960401, PUPT-1615, quant-ph/9604035.
- [15] D. A. Meyer, “Quantum lattice gases and their invariants”, UCSD preprint.
- [16] P. A. M. Dirac, *The Principles of Quantum Mechanics*, fourth edition (Oxford: Oxford University Press 1958).
- [17] H. Weyl, *The Theory of Groups and Quantum Mechanics*, translated from the second (revised) German edition by H. P. Robertson (New York: Dover 1950).
- [18] G. Zanetti, “Hydrodynamics of lattice gas automata”, *Phys. Rev. A* **40** (1989) 1539–1548;
 Z. Cheng, J. L. Lebowitz and E. R. Speer, “Microscopic shock structure in model particle systems: The Boghosian-Levermore cellular automaton revisited”, *Commun. Pure Appl. Math.* **XLIV** (1991) 971–979;
 B. Hasslacher and D. A. Meyer, “Lattice gases and exactly solvable models”, *J. Stat. Phys.* **68** (1992) 575–590.
- [19] W. L. Briggs and V. E. Henson, *The DFT: An owner’s manual for the discrete Fourier transform* (Philadelphia: SIAM 1995).
- [20] G. ’t Hooft, “Equivalence relations between deterministic and quantum mechanical systems”, *J. Stat. Phys.* **53** (1988) 323–344.
- [21] J. C. Slater, *Quantum Theory of Matter* (New York: McGraw-Hill 1951) Chapter 10.
- [22] D. A. Meyer, “Quantum mechanics of lattice gas automata. II. Boundary conditions and other inhomogeneities”, UCSD/IPS preprint.

- [23] T. Ando, A. B. Fowler and F. Stem, “Electronic properties of two-dimensional systems”, *Rev. Mod. Phys.* **54** (1982) 437–672;
D. K. Ferry and H. L. Grubin, “Modeling of quantum transport in semiconductor devices”, in H. Ehrenreich and F. Spaepen, eds., *Solid State Physics: Advances in Research and Applications* **49** (1995) 283–448;
and references therein.
- [24] D. A. Meyer, in preparation.